OPTOELECTRONICS AND ADVANCED MATERIALS – RAPID COMMUNICATIONS Vol. 1, No. 7, July 2007, p. 348 - 352

Stabilized mode locked fiber laser

M. K. ISLAM[a,*], M. ZAFRULLAH[a], P. L. CHU[b]
[a]*Faculty of Telecommunication and Information Engineering, University of Engineering and Technology, Taxila, 47050, Pakistan*
[b]*Optoelectronics Research Centre, City University of Hong Kong*

Generation of ultra short pulses is of great importance for applications in optical signal processing, communications, high-speed electronics, and time resolved study of many physical, chemical and biological processes. However, it is desirable to be able to generate these pulses at an arbitrary repetition rate with high stability. The pulse instability in figure-eight fiber lasers can be removed by introducing intentional twist in the fiber, which provides a controllable birefringence-induced phase-bias. The proposed theory has been verified experimentally. The stabilized laser can generate very stable pulses with the wavelengths tunable by simply adjusting the polarization controllers in the two loops of a figure-eight laser. The stability of the laser has been analyzed quantitatively by using RF spectrum analysis of the mode-locked pulse train. Fluctuations in pulse repetition time and in pulse energy as well as jitter in pulse width occur simultaneously. All these types of noise have been characterized quantitatively by examining the higher harmonics of the RF spectrum. By optimizing the total dispersion and cavity length of the laser, it was found by measurement that a peak to peak stability of 99.2% and a timing jitter of 5.59 psec for 2.31 MHz pulse train were obtained. However, it is observed that the variation of cavity parameters results in increased timing jitter and peak pulse instability.

(Received June 8, 2007; accepted July 9, 2007)

Keywords: Birefringence, Laser stability, Optical fiber laser, Optical pulse generation, Optical solitons

1. Introduction

There are various techniques of generating short optical pulses but gain switching and mode locking are the two commonly used methods. In mode locking, an intra cavity gain, loss, or phase element is used to lock the longitudinal modes into some physical relationship in order to produce short optical pulses. Mode locked fiber lasers employing rare earth doped element, as a gain medium are important systems for the generation of short, high power optical pulses. Passive mode-locked fiber lasers have been the subject of intensive investigations because of their attractive prospect of an easy-to-use optical short pulse source [1-7]. Many other short pulse sources have been demonstrated using various configurations [8-10].

Fiber laser, as a source of short pulse generation finds applications in telecommunications and optical signal processing, where, low noise and stable pulse train is the main requirement. However, fiber lasers do have certain limitations. They are subject to environmental changes; timing jitter and shot to shot instability. Irrespective of the laser geometry, with subpicosecond operation the lasers do not exhibit a strictly periodic output. Also the appearance of down shifted and up shifted spectral components (side bands) limits the pulse width and deteriorates the pulse quality. Furthermore, it is difficult to achieve high-energy short pulses from these lasers. The fluctuations in pulse repetition time and in pulse energy as well as jitter in pulse width occur simultaneously in fiber lasers. The potential of mode-locked fiber lasers will be enhanced if their stability is ensured against various environmental perturbations. This instability has been attributed to the sensitivity of the birefringence of the fiber in the nonlinear amplifying loop mirror (NALM) to the environment such as temperature change, accidental applied pressure and unintentional bending etc. [5]. Many techniques have been exploited to stabilize mode locked fiber lasers by using additional elements in the cavity. We present a simple method which requires a birefringence bias to stabilize the laser. By introducing a gradual twist in the fiber, a stable pulse train is generated from a figure-eight fiber laser. Although, various methods have been employed to generate a stable, high-energy pulse train from mode locked fiber lasers, but quantitative stability analysis of these lasers is deficient.

Before exploiting any application of the fiber laser, it is important to analyze the stability of the laser. We have analyzed the timing jitter and shot to shot pulse stability of this laser quantitatively by examining its RF spectrum of fundamental and higher harmonics. The cavity parameters can be optimized for designing a stable pulse train mode locked laser.

2. Theory

The pulse instability in the fiber laser is caused by the environmental effect on the birefringence of the fiber loop. The dominant effect is due to the incidentally applied pressure on the fiber which introduces a random birefringence. To reduce this effect, we introduce a deliberate but constant and large birefringence to the fiber which swarms the random birefringence due to pressure. A gradual twist to the fiber has also been used in the stabilization of the cw wavelength of a ring fiber laser [11].

The passive mode locking in a NALM is given by the maximization of its reflectivity which can be expressed as [12]:

$$R = 2\alpha(1-\alpha)\left[1+\sqrt{\gamma_s^2+\gamma_a^2}\cos(\phi_{NR}-\varepsilon)\right] \quad (1)$$

where α is the coupling ratio of the 3dB coupler, ϕNR is the nonreciprocal phase shift and is given by:

$$\phi_{NR} = \frac{2\pi n_2 L}{\lambda}|E|^2 (g-1) \quad (2)$$

Where L is the total length of the loop, g is the gain of the fiber amplifier, n_2 is the nonlinear index coefficient of silica glass, λ is the operating wavelength, and E is the electric field of the pulse.

The parameters γ_a, γ_s, and ε are related to the Jones matrix B of the NALM [12]:

$$\gamma_a = -\operatorname{Im}\left\{\vec{\chi}_{in}{}^* B^* B\vec{\chi}_{in}\right\} \quad (3)$$

$$\gamma_a = -\operatorname{Re}\left\{\vec{\chi}_{in}{}^* B^* B\vec{\chi}_{in}\right\} \quad (4)$$

$$\tan\varepsilon = \gamma_a / \gamma_s \quad (5)$$

To find the Jones matrix B, we assume that the fiber loop is composed of three birefringent elements, i.e. the polarization controller, the twist, and the applied pressure. The polarization controller behaves like a half wave plate with the polarization axes oriented at an angle θ from the fixed laboratory coordinates. Rotating the polarization controller means changing θ. Thus the Jones matrix for the polarization controller is given by:

$$P = \begin{bmatrix} -j\cos 2\theta & j\sin 2\theta \\ j\sin 2\theta & j\cos 2\theta \end{bmatrix} \quad (6)$$

If the fiber is twisted with a rate T, its Jones matrix is:

$$S = \begin{bmatrix} \cos TL & -\sin TL \\ \sin TL & \cos TL \end{bmatrix} \quad (7)$$

If a force F is applied diametrically across the fiber cross-section, it introduces a compressive stress σ_y in the direction of the applied force such that,

$$\sigma_y = -\frac{6F}{\pi d} \quad (8)$$

where d is the overall diameter of the fiber. Here, the UV acrylate coating has been ignored. The birefringence generated by the applied force can then be calculated by taking into account of the photoelastic coefficients of silica glass:

$$n_x - n_y = \frac{3.458\times 10^{-5}\times 6F}{\pi d} \quad (9)$$

If the force F is applied over a length ℓ in the fiber, the phase retardation between the two polarizations of light is:

$$\Gamma = \frac{2\pi\ell}{\lambda}(n_x - n_y) \quad (10)$$

If the force is applied vertically so that its polarization axes coincide with those of the laboratory coordinates, the Jones matrix can be written as:

$$W = \begin{bmatrix} e^{-j\Gamma/2} & 0 \\ 0 & e^{j\Gamma/2} \end{bmatrix} \quad (11)$$

Thus the Jones matrix due to the overall polarization change in the NALM is given by:

$$B = PWT = \begin{bmatrix} b_{11} & b_{12} \\ b_{21} & b_{22} \end{bmatrix} \quad (12)$$

Where

$$b_{11} = 0.5\begin{bmatrix} -\cos(2\theta+TL-\Gamma/2)-\cos(2\theta+TL+\Gamma/2) \\ +\, j\sin(2\theta-TL+\Gamma/2)-\, j\sin(2\theta-TL-\Gamma/2) \end{bmatrix}$$

$$b_{12} = 0.5\begin{bmatrix} \sin(2\theta-TL+\Gamma/2)+\sin(2\theta-TL-\Gamma/2) \\ +\, j\cos(2\theta+TL-\Gamma/2)-\, j\cos(2\theta+TL+\Gamma/2) \end{bmatrix}$$

$$b_{21} = 0.5\begin{bmatrix} \sin(2\theta+TL+\Gamma/2)+\sin(2\theta+TL-\Gamma/2) \\ -\, j\cos(2\theta-TL-\Gamma/2)+\, j\cos(2\theta-TL+\Gamma/2) \end{bmatrix}$$

$$b_{22} = 0.5\begin{bmatrix} \cos(2\theta+TL-\Gamma/2)+\cos(2\theta+TL+\Gamma/2) \\ +\, j\sin(2\theta+TL+\Gamma/2)-\, j\sin(2\theta-TL-\Gamma/2) \end{bmatrix}$$

Thus, from the bij elements of the Jones matrix, we can see that the fiber twist introduces a phase bias which, if large enough, can make the contribution Γ/2 from the applied force negligible. For example, in the experimental figure-eight laser, for a loop length of the NALM equal to 60 m and a twist rate of 1°/cm is introduced. This gives a total phase shift TL=6000° or 104.7 rad. On the other hand, if a 1 gm force is applied across 1mm long fiber, the resulting phase shift is Γ=2.19 rad. Hence, twisting the fiber has the effect of stabilizing the pulse from the figure-eight laser. Also, the increase in the birefringence added to the system can results in dual wavelength/dual polarization harmonic mode locked lasing.

3. Experiment

The schematic of figure-eight laser cavity is shown in Fig. 1. The NALM of the figure eight laser constructed in our laboratory has 10m of Erbium-doped fiber (EDF) with Erbium concentration 730 ppm and co-doped with 20300 ppm of Al. Its mode field diameter is 4.9 μm and dispersion +0.5 ps/nm/km at λ=1560 nm. This fiber is joined to a length of 50 m dispersion shifted fiber (DSF) which has the zero dispersion wavelength of 1540 nm. This connected fiber is wound onto a drum with a twist approximately 1°/cm. A polarization controller is inserted between the DSF and the 3dB coupler. A 1480 nm semiconductor pump laser delivering an optical power up to 80 mW is connected to the EDF via a WDM coupler. The other input port of this coupler is connected to the other output port of the 3 dB coupler. The linear loop of the figure-eight laser consists of 10 m DSF connected to a polarization controller at one end and an isolator at the other end. An output 90:10 fiber coupler is connected between the isolator and the 3dB coupler. The length of the linear loop is 20 m, and the total cavity length is 90 m.

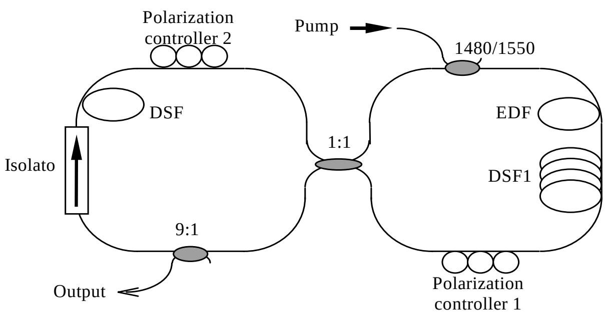

Fig. 1.The schematic of figure-eight laser.

The output pulse of this laser can be adjusted by rotating the angles of the polarization controllers in the NALM and in the linear loop. This is equivalent to adjusting the birefringence bias ε in equation (5) which leads to a particular mode locking condition.

Thus at one setting of the controllers, The pedestal free optical spectrum with FWHM of 25 nm measured with a resolution of 0.1 nm revealing the negligible cw background is shown in Fig. 2. The corresponding autocorrelation trace recorded by Inrad 5-14-LDA with a measured pulse width of 125 fs assuming sech 2 shape is shown in Fig. 3.

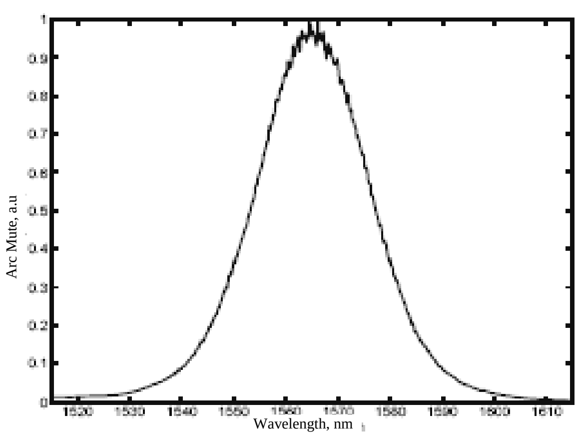

Fig. 2. Optical spectrum of the mode locked pulse.

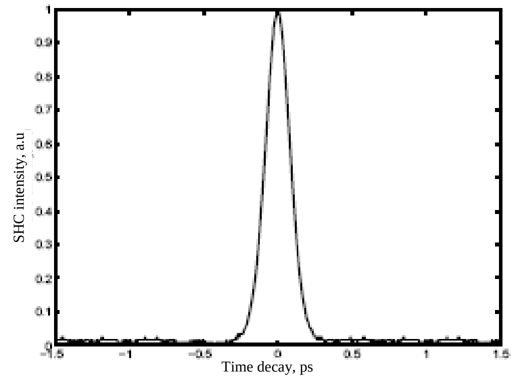

Fig. 3. Autocorrelation of the mode locked pulse.

The time-bandwidth product of 0.38 is very close the theoretical transform limit of a soliton. The pulse peak power of 4 kW and energy of 0.5 nJ corresponds to the measured average output power of 1.2 mW. Stable pulse train when the laser was in operation for few hours is shown in Fig. 4. By adding more birefringence through adjustment of the polarization controllers, laser can result in dual wavelength harmonic mode locked operation [13].

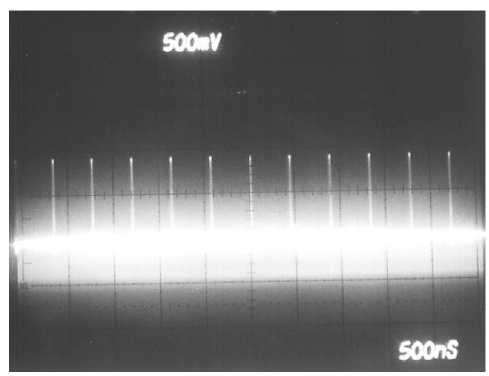

Fig. 4. Stable mode locked pulse train.

4. Stability analysis

The stability of the pulse source must be questioned before using it for any application. The fluctuations of the pulse energy, pulse repetition time, and pulse duration can be gained from analysis of the fundamental and higher harmonics of the RF spectrum [14]. All these types of noise can be characterized individually in a quantitative way, even if they occur simultaneously. Each harmonic consists of the sum of a constant amplitude noise spectrum, which is due to the pulse energy fluctuations, and a component from pulse width fluctuations, and timing jitter which increases as the square of the harmonic number [15].

The microwave spectra of the fundamental and 30th harmonic over a span of 80 kHz with bandwidth resolution of 300 Hz, measured by an HP 8591A spectrum analyzer are shown in Fig. 5 and Fig. 6, respectively.

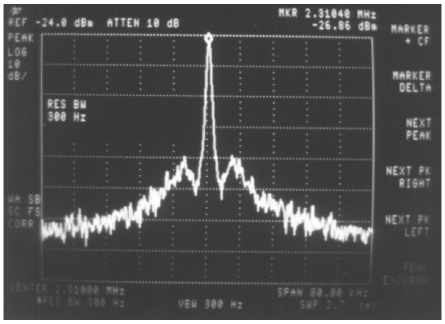

Fig. 5. RF spectrum at fundamental frequency.

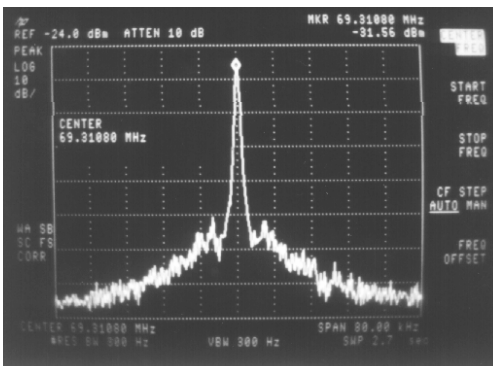

Fig. 6. RF spectrum of 30th harmonic.

The fluctuations in pulse energy can be calculated from the fundamental component of the RF spectrum as [11],

$$\frac{\Delta E}{E} = \sqrt{\left(\frac{P_c}{P_a}\right)_f \frac{\Delta f_a}{\Delta f_{res}}} \tag{13}$$

where P_c and P_a are the maxima of the noise band and the signal respectively, subscript f stands for fundamental frequency. Δf_a and Δf_{res} is the full width half maximum of the noise floor and spectral resolution of the spectrum analyzer respectively. The energy fluctuation calculated for our laser is only 0.8%. The very high amplitude stability is quite remarkable.

The timing jitter can be easily calculated from a higher harmonics [11],

$$\frac{\Delta t}{T} = \frac{1}{2\pi n}\sqrt{\left(\frac{P_b}{P_a}\right)_f \frac{\Delta f_j}{\Delta f_{res}}} \tag{14}$$

where T is the cavity round trip time, Δt is the timing jitter, n is the harmonic order of the frequency component, P_b is the power of the noise floor responsible for jitter, Δf_j is the bandwidth of the corresponding noise component. From the 100th harmonic, shown in Fig. 7, we can easily calculate for Δf_j = 20kHz, the ratio $\Delta t/T = 1.23\times10^{-5}$. For a repetition rate of 2.31 MHz, the timing jitter is 5.59 ps which give the shot to shot pulse fluctuations of only 0.0129%.

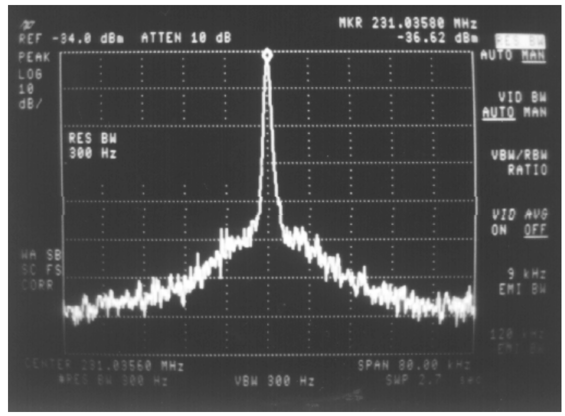

Fig. 7. RF spectrum of 100th harmonic.

It was observed that when a mode-locked laser is unstable, its RF spectrum has some spurious sidebands around the fundamental and higher harmonics. However, when the laser was stabilized, the spurious sidebands completely disappear. From the spectra shown in the above figures, it can be seen that there are no spurious side bands around the fundamental and higher harmonics of the RF spectrum. This reveals the high stability of the laser pulses.

When the laser is destabilized intentionally by changing the cavity parameters, i.e. dispersion shifted fiber in the cavity is reduced to a shorter length, the laser is still mode-locked with apparently a stable pulse train as shown in Fig. 8, however, RF spectrum shows high amplitude of spurious side bands as shown in Fig. 9; which results in high peak to peak variations and timing jitter.

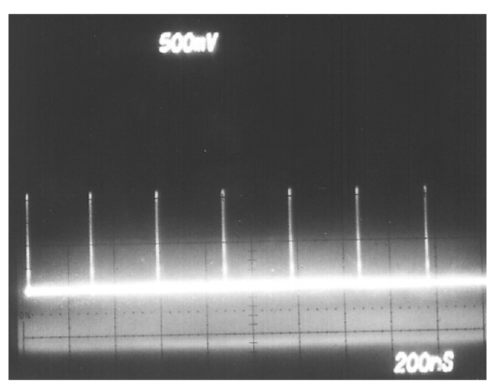

Fig. 8. Mode locked pulse train.

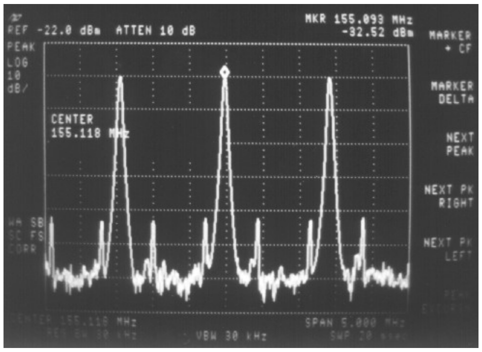

Fig. 9. RF spectrum.

5. Conclusion

We have shown both theoretically and experimentally that the pulses generated by the figure-eight laser can be stabilized by the introduction of twist in the fiber loop. Once this is achieved, the pulse train can be tuned over a range of 4 nm by adjusting the polarization controllers in the loop which is equivalent to setting different passive locking conditions. The stability of the mode locked laser is investigated by examining the corresponding RF spectrum for the fundamental and higher harmonics.

References

[1] J. W. Nicholson, S. Ramachandran, S. Ghalmi, Optics Express **15**(11), 6623 (2007).

[2] J. W. Nicholson, M. Andrejco, Optics Express **14**(18), September (2006).

[3] N. H. Seong, Dug Y. Kim, IEEE Photonics. Tech. Lett. **14**(4), April (2002).

[4] S. Tzelepis, S. Markatos, Th. Kalpogiannis, Sphicopoulos, C. Caroubalos, J. Lightwave Technol. **11**(11), 1729 (1993).

[5] Duling, III, “Subpicosecond All-Fiber Erbium Laser,” Electron. Lett. **27**(6), 544 (1991).

[6] Richardson, R. I. Laming, D. N. Payne, V. J. Matsas, M. W. Phillips, Electron. Lett. **27**(16), 1451 (1991).

[7] Wu, J. Strait, R. L. Fork, Opt. Lett. **18**(17), 1444 (1993).

[8] N. Pandit, D. U. Noske, J. R. Taylor, J. Mod. Opt. **41**(1), 11 (1994).

[9] W. H. Loh, A. B. Grudinin, D. N. Payne, Electron. Lett. **30**(5), 413 (1994).

[10] V. J. Matsas, T. P. Newson, D. J. Richardson, D. N. Payne, Electron. Lett. **28**(15), 1391 (1992).

[11] C. X. Shi, Optics Communications **125**, 349 (1996).

[12] W. Y. Oh, B. Y. Kim, H. W. Lee, IEEE J. Quantum Electronics **32**(2), 333 (1996).

[13] T. O. Tsun, M. K. Islam, P. L. Chu, Opt. Comm. **141**, August 1997.

[14] D. Von der Linde, Appl. Phys. B, **39**, 201 (1986).

[15] I. G. Fuss, IEEE J. Quantum Electron. **30**, 2707 (1994).

*Corresponding author: Drmkisalm@uettaxila.edu.pk